HHS Public Access

Author manuscript

Genes Chromosomes Cancer. Author manuscript; available in PMC 2024 April 01.

Published in final edited form as:

Genes Chromosomes Cancer. 2023 April ; 62(4): 191–201. doi:10.1002/gcc.23102.

Malignant Undifferentiated Epithelioid Neoplasms with *MAML2* rearrangements: a Clinicopathologic Study of Six Cases Demonstrating a Heterogenous Entity

Josephine K. Dermawan[1], **Sara E. DiNapoli**[1], **Purvil Sukhadia**[1], **Kerry A. Mullaney**[1], **Rebecca Gladdy**[2], **John H. Healey**[3], **Abbas Agaimy**[4], **Arjen H. Cleven**[5,6], **Albert J.H. Suurmeijer**[5], **Brendan C. Dickson**[7], **Cristina R. Antonescu**[1]

[1]Department of Pathology and Laboratory Medicine, Memorial Sloan Kettering Cancer Center, New York, NY, USA

[2]Department of Surgery, Sinai Health System, Toronto, Ontario, Canada

[3]Department of Surgery, Memorial Sloan Kettering Cancer Center, New York, NY, USA

[4]Institute of Pathology, Erlangen University Hospital, Comprehensive Cancer Center, European Metropolitan Area Erlangen-Nuremberg, Friedrich Alexander University of Erlangen-Nuremberg, Erlangen, Germany

[5]Department of Pathology, University Medical Center Groningen, Groningen, The Netherlands

[6]Department of Pathology, Leiden University Medical Center, Leiden, The Netherlands

[7]Department of Laboratory Medicine and Pathology, University of Toronto, Toronto, Ontario, Canada

Abstract

Among mesenchymal tumors, *MAML2* gene rearrangements have been described in a subset of composite hemangioendothelioma and myxoinflammatory fibroblastic sarcoma (MIFS). However, we have recently encountered *MAML2*-related fusions in a group of 6 undifferentiated malignant epithelioid neoplasms that do not correspond to any established pathologic entities. The patients included 5 males and 1 female, aged 41–71 years old (median 61 years). The tumors involved the deep soft tissue of extremities (hip, knee, arm, hand), abdominal wall, and the retroperitoneum. Microscopically, the tumors consisted of solid sheets of highly atypical epithelioid cells with abundant cytoplasm and showed prominent mitotic activity and necrosis. In 3 cases, the cells displayed hyperchromatic nuclei or conspicuous macronucleoli and were admixed with

Corresponding author: Cristina R. Antonescu, MD, Department of Pathology, Memorial Sloan Kettering Cancer Center, 1275 York Avenue, New York, NY 10065, antonesc@mskcc.org.

Author Contribution Statement

JKD performed study design, data acquisition and interpretation, writing and revision of the paper. SD, KM, PS, RG, JH, AA, AC, AJHS, and BCD performed data acquisition and critical review of the paper. CRA performed study design and conception, analysis and interpretation of data, writing, review and revision of paper. All authors read and approved the final manuscript.

Ethics Approval / Consent to Participate

This study was approved by the Memorial Sloan Kettering Cancer Institute Institutional Review Board.

Conflict of Interest Statement

All authors report no conflict of interests related to this study.

background histiocytoid cells and a lymphoplasmacytic infiltrate. By immunohistochemistry (IHC), the neoplastic cells had a nonspecific phenotype. On targeted RNA sequencing, *MAML2* was the 3' partner and fused to *YAP1* (3 cases), *ARHGAP42* (2 cases), and *ENDOD1* (1 case). One case with *YAP1::MAML2* showed strong and diffuse nuclear YAP1 immunostaining and harbored a concurrent *RBMS3::RAF1* fusion. In 2 cases with targeted DNA sequencing, mutations in *TP53*, *RB1* and *PTEN* were detected in 1 case, and *PDGFRB* mutations, *CCNE1* amplifications and *CDKN2A/2B* deletion were detected in another case, which showed strong and diffuse PDGFRB expression by IHC. Of the 4 cases with detailed clinical history (median follow-up period 8 months), 3 developed distant metastatic disease (one of which died of disease); one case remained free of disease 3 years following surgical excision. In conclusion, we describe a heterogeneous series of *MAML2*-rearranged undifferentiated malignant epithelioid neoplasms, a small subset of which may overlap with a recently described MIFS variant with *YAP1::MAML2* fusions, further expanding the clinicopathologic spectrum of mesenchymal neoplasms with recurrent *MAML2* gene rearrangements.

Keywords

MAML2; YAP1; undifferentiated sarcoma; epithelioid; myxoinflammatory fibroblastic sarcoma

INTRODUCTION

Mastermind-like (MAML) was first identified as a pivotal coactivator of Notch-dependent transcription and belongs to a group of proteins encoded by the eponymous *MAML* genes: *MAML1, MAML2* and *MAML3*. MAML2 (mastermind-like 2) is a key regulator of various signaling pathways that are essential for developmental processes as well as tumorigenesis, including Notch, nuclear factor-κB (NF-κB), and β-catenin signaling.[1–4]

Recurrent gene rearrangements of *MAML2* have been described in mucoepidermoid carcinoma,[5] poromas/porocarcinoma,[6] metaplastic thymoma,[7] retiform and composite hemangioendothelioma,[8–10] and a rare "nodular necrotizing" variant of myxoinflammatory fibroblastic sarcoma (MIFS).[11] Herein, we report a series of six undifferentiated sarcomas characterized by an epithelioid morphology and the presence of recurrent *MAML2* gene rearrangements with various fusion partners.

Materials and Methods

Study Cohort

Archival files from the Memorial Sloan Kettering Cancer Center Department of Pathology, as well as the personal consultation files of the authors (BCD, AJHS, CRA), were reviewed and searched for cases with *MAML2* gene rearrangement. Clinical data, including age, sex, and anatomic site were retrieved from pathology reports. Hematoxylin and eosin–stained slides from resection specimens were rereviewed. Histopathologic parameters, including architectural patterns, cytomorphology, degree of cytologic atypia, mitotic activity, and tumor necrosis were evaluated. The study was approved by the Institutional Review Board.

Immunohistochemical staining

The relevant antibodies and the dilutions used in this study are as follows: BRG1 (Santa Cruz Technology clone B-7, 1:250), CD163 (Ventana clone MRQ-26, undiluted), CD31 (Ventana clone JC70, undiluted), CD34 (Ventana clone QBEnd10, undiluted), CDK4 (Invitrogen, clone DCS-31, 1:200), desmin (Ventana clone DE-R-11, undiluted), EMA (Ventana clone DE-R-11, undiluted), ERG (Ventana clone E29, undiluted), INI1 (BD Bioscience clone BAF47, 1:200), MDM2 (Millipore clone IF2, 1:50), NUT (Cell Signaling Technology, clone C52B1, 1:100), S100 (Cell Marque clone 4C4.9, 1:600), SMA (Cell Marque clone 1A4, undiluted), SOX10 (Biocare clone BC34, 1:50), and YAP1 (Santa Cruz Technology clone 63.7, 1:1000).

Targeted DNA and RNA Sequencing

For targeted RNA sequencing, an anchored multiplex PCR-based assay (MSK-Fusion) (cases 1, 2, 4, 5, 6) and the TruSight RNA fusion panel (Illumina, San Diego, CA) (cases 3, 5) were used.[13–15] The former is a custom amplicon-based NGS assay using the Archer FusionPlex (Archer, Boulder, CO) standard protocol targeting specific exons in 123 genes, requiring a minimum of 5 unique reads and 3 reads with unique start sites for each fusion call.[14] The latter is a hybrid capture-based assay that targets 507 known fusion-associated genes.[15,16] Detailed descriptions of MSK-IMPACT (performed in cases 1 and 2), a hybridization capture-based targeted DNA NGS assay of 505 cancer genes, were described previously.[13] Unstained recut slides from archival formalin-fixed, paraffin-embedded (FFPE) blocks were used for sequencing following extraction of DNA and RNA. For mRNA levels, for samples tested on the Illumina panel, the average read counts across the transcript from the bam files were obtained by manual inspection on integrated genome viewer; for samples tested by the Archer panel, the RNA expression levels were provided by the Archer proprietary platform and were arbitrary values normalized to the average expression of Archer's internal control.

Results

Clinical summary

The cohort consisted of 5 males and 1 female, aged 41 to 71 years old (median 60.5 years). The primary sites of involvement included the extremities (hip, knee, arm, hand) in four patients, the abdominal wall (multifocal lesions) in one patient, and the retroperitoneum in another patient. All tumors occurred in the deep soft tissues, including skeletal muscle, and ranged between 1.3 to 14.8 cm in greatest dimensions (median 5.0 cm) (Figure 1A–B, E–F). For the four cases with detailed clinical data (cases 1, 2, 4, 5): the patients underwent surgical excision and/or neoadjuvant/adjuvant chemotherapy. Over a limited median follow-up period of 8 months (range 2 to 36 months), three of four patients developed distant lung (cases 1, 2, 5) and bone/soft tissue (case 2) metastases (Figure 1C–D), of which two remained alive with disease (cases 1, 5) and one died of disease (case 2). One patient remained free of disease 36 months following surgery (case 4). The detailed clinical presentation and follow-up information is presented in Table 1.

Histopathologic features

Microscopically, all 6 cases consisted of cellular, high-grade, and predominantly epithelioid cells arranged in solid sheets and/or fascicles. Nuclear pleomorphism ranged from mild to moderate. The neoplastic cells displayed abundant eosinophilic to amphophilic cytoplasm and enlarged nuclei with hyperchromatic to vesicular chromatin (Figure 2A–F). In two cases (cases 4 and 5) located in the hand and knee, the neoplastic cells displayed virocyte-like macronucleoli and were scattered among background histiocytoid cells admixed with a prominent mixed inflammatory infiltrate including neutrophils, eosinophils and lymphocytes, resembling MIFS (Figure 3A–E). In one case (case 6) located in the arm, set in an extensively hyalinized/necrotic background, the epithelioid/histiocytoid neoplastic cells displayed hyperchromatic, irregular nuclei and eosinophilic, vacuolated cytoplasm. The hyalinized areas were rimmed by lymphoid tissue, imparting the appearance of lymph node involvement (Figure 3F–G). Mitotic activity was conspicuous and greater than 20 per 10 high power fields in 3 of 6 cases. Tumor necrosis was present in all cases ranging from focal in 3 cases to extensive (> 50%) in 3 cases. Hemosiderotic fibrolipomatous tumor (HFLT)-like areas were not identified in any of the cases. The histopathologic features are summarized in Table 2.

Immunohistochemical summary

Immunohistochemically, the tumors showed an undifferentiated phenotype with mostly nonspecific staining of patchy to focal SMA/desmin and cytokeratins, but were negative for melanocytic, vascular, hematolymphoid markers and retained INI1 and BRG1 expression. Interestingly, in case 5, where *MAML2* was fused to *YAP1*, the N-terminal YAP1 immunohistochemical antibody was highly expressed diffusely in the tumor nuclei (Figure 3H). In case 2, where there was a concurrent *PDGFRB* mutation, the neoplastic cells also express strong and diffuse membranous PDGFRB staining (Table 3).

Molecular findings

By RNA sequencing, *MAML2* rearrangement was detected in all six cases. The 5’ partners were *ARHGAP42* (case 1, 3), *ENDOD1* (case 2), and *YAP1* (cases 4–6). *MAML2* and all three of its 5’ partners are in proximity to each other on chromosome 11q21-q22 (Figure 4A). All fusions were predicted to be in-frame and involved exons 2 and 3 of *MAML2* (NM_003403.4). As the 3’ partner, the transcriptional factor IIA (TFIIA) domain of MAML2 is preserved in the predicted chimeric protein (Figure 4B). Interestingly, in case 5 a concurrent fusion *RBMS3::RAF1* with adequate read support (339 reads spanning breakpoint, 66 unique start sites by Archer) and its reciprocal fusion *RAF1::RBMS3* were also detected. The presence of concurrent *YAP1::MAML2* and *RBMS3::RAF1* fusions in case 5 was confirmed independently by an amplicon-based, anchored multiplex PCR targeted RNA sequencing assay and a hybrid capture-based Illumina TruSight RNA fusion assay (Dickson 2018).[13,15] *VGLL3* RNA expression was upregulated in case 5 but not upregulated in cases 1, 2 or 6 (not available for evaluation for cases 3 and 4). *MAML2* expression was not upregulated in cases 1, 2, 4, 5 or 6 (not available for evaluation for case 3).

Targeted DNA sequencing data by MSK-IMPACT was available for cases 1 and 2. Case 1 had a tumor mutation burden (TMB) of 4.1 mutations per megabases (mt/Mb), and harbored missense mutations in *TP53* (p.Y234C), *BRCA2* (p.A2351P), and *PREX2* (p.N64T), a truncating frameshift mutation in *RB1* p.A538Qfs*5, and an intragenic deletion in *PTEN*. Case 2 had a TMB of 6.6 mt/Mb, and harbored *PDGFRB* mutations in exon 11 (p.I547_I553dup) and exon 18 (p.R853P), copy number amplifications on 19p13.2 (contains *CCNE1*, *BRD4*, *NOTCH3*) and deletions on 9p21.3 (contains *CDKN2A/CDKN2B*). These two cases showed no amplification at chromosome 3p11–12 (where *VGLL3* is located) by copy number profiling. Details of the molecular findings are described in Table 3.

DISCUSSION

We report six cases of undifferentiated malignant epithelioid neoplasms with *MAML2* gene fusions arising in the deep soft tissues. In our cohort, the 5' partner of *MAML2* were *YAP1*, *ARHGAP42* and *ENDOD1*, the latter two have not been previously reported as a fusion partner of *MAML2*. Interestingly, all these genes are located on the same or adjacent bands on chromosome 11: *MAML2* and *ENDOD1* on 11q21; *YAP1* and *ARHGAP42* on 11q22. In the predicted chimeric proteins, *MAML2* retains the C-terminal TFIIA domain, preserving its function as a transcriptional coactivator.[2–4] Additionally, a recent study identified a PPxY motif in MAML1 and MAML2 that interacts with YAP1 or TAZ (WWTR1) and promotes their nuclear localization, where MAML1 and MAML2 also act as a transcriptional coactivator in the nucleus, thereby promoting oncogenic transformation.[17] As YAP1 retained its N-terminal portion in the chimeric protein, it showed high expression by immunohistochemistry in case 5 using an antibody that recognizes its N-terminal in the case with *YAP1::MAML2*, where the oncogenic fusion driver is predicted to be overexpressed. Of note that this is the reverse scenario as seen in *YAP1::TFE3* epithelioid hemangioendothelioma, where the loss of C-terminal YAP1 immunostaining is detected for the diagnosis.[18]

The two cases (cases 4, 5) of this study with *YAP1::MAML2* that were located on the hand, and knee and displayed sheets of epithelioid cells with large vesicular nuclei and prominent virocyte-like macronucleoli admixed with a mixed inflammatory infiltrate—histopathologic features that overlap with the recently described "nodular necrotizing" variants of MIFS with recurrent *YAP1::MAML2* fusions.[11] In an additional case (case 6, arm) the tumor cells were associated with extensive hyalinization and necrosis centrally and surrounded at the periphery by lymphoid aggregates. However, in the study by Perret et al, only 2 of 7 cases were acral location, and they did not comment on whether any of their cases showed HFLT-like areas. In the current study, only one case occurred in acral location (harboring *YAP1-MAML2* fusion), and none of our cases showed a nodular configuration or HFLT-like areas, i.e., mixture of mature adipose tissue and bland spindled cells admixed with abundant hemosiderin and background histiocytes away from the main tumor. MIFS, as well as the related HFLT, was first described to harbor rearrangements of *TGFBR3* and *MGEA5* as a result of translocations between chromosomes 1 and 10 and amplification of *VGLL3* gene on 3p11–12.[19–22] Later, recurrent *BRAF* rearrangements have also been described in MIFS but not HFLT.[23] The genetic heterogeneity of the MIFS spectrum begs the question of whether these *MAML2*-rearranged tumors should be grouped under the same umbrella of

MIFS, based on their limited clinical, morphologic and molecular overlap. Further studies are needed to investigate the pathogenetic relationship between these tumors and “MIFS family” including transcriptional and epigenetic platforms.

On the other hand, in a recent study of MIFS using array comparative genomic hybridization (array CGH), *VGLL3* amplification was seen in 8 (40%) of 20 cases of MIFS, regardless of whether these cases harbored t(1;10) or *BRAF* rearrangements.[22] *VGLL3* amplification is also strongly correlated with upregulation of *VGLL3* RNA expression level.[24] In the study by Perret et al, the 4 cases with array CGH showed flat copy number profiles (including 3p11–12 where *VGLL3* is located), and the single case with FISH showed no *VGLL3* amplification.[11] In our study, only one case (case 5, knee) showed evidence of upregulation of *VGLL3* RNA expression. All these features cast uncertainty on the diagnosis of MIFS for *MAML2*-rearranged malignant epithelioid neoplasms. Furthermore, the first three cases in our cohort did not exhibit histologic or clinical features of MIFS and were essentially undifferentiated sarcomas with an epithelioid morphology. Moreover, in contrast to the complete lack of local recurrence or distant metastases in the study by Perret et al,[11] the highly aggressive clinical behavior in all except one patient with available follow-up developing distant spread in the current study is not consistent with the biology of MIFS. In fact, the only patient without tumor progression had an acral lesion harboring *YAP1-MAML2* (case 4) and displaying a partial morphologic overlap with MIFS. The fact that oncogenic mutations in *TP53*, *BRCA2*, *RB1*, etc., copy number losses in *PTEN* and *CDKN2A/2B*, and copy number gains in *CCNE1* were also detected in these tumors, coupled with the relatively high TMB of 4 to 6 mt/Mb—a profile akin to other high-grade sarcomas.[25]

Moreover, it is intriguing that one of the cases from the study by Perret et al describing a “nodular necrotizing” variant of MIFS with *YAP1::MAML2* also showed a concurrent *BRAF* rearrangement, whereas one of the cases with *YAP1::MAML2* in the current study (case 5) had a concurrent *RAF1* rearrangement. The concurrent *YAP1::MAML2* and *RBMS3::RAF1* fusions in case 5 were confirmed independently by two different targeted RNA sequencing assays (amplicon-based and hybrid capture based). In almost all tumors, one dominant driver fusion is sufficient to induce oncogenic transformation. Thus, it is highly unusual for sarcomas to harbor two concurrent driver fusions. The biological relevance of this rare phenomenon remains to be investigated.

Additionally, recurrent *MAML2* fusions have been described in rare cases of retiform and composite hemangioendothelioma (CHE) with neuroendocrine differentiation.[8–10] Although this type of CHE may show severe nuclear atypia, they also display areas with clear vascular differentiation and consistently express vascular markers such as ERG, CD31 and CD34. Additionally, *MAML2* rearrangements are known to be recurrent in certain carcinomas including mucoepidermoid carcinoma (*CRTC1::MAML2*),[5] metaplastic thymomas (*YAP1::MAML2*),[7] and poromas/porocarcinomas (*YAP1::MAML2*),[9] which have specific clinicopathologic features that do not overlap with the *MAML2*-rearranged undifferentiated malignant neoplasm in this study.

The differential diagnosis of *MAML2*-rearranged undifferentiated malignant neoplasm is broad and includes any high-grade sarcomas with epithelioid morphology as well as undifferentiated malignant neoplasms. Proximal-type epithelioid sarcoma also consists of solid sheets of large epithelioid cells with abundant glassy eosinophilic cytoplasm and enlarged nuclei that is eccentrically placed, imparting a rhabdoid cytomorphology. Immunophenotypically, epithelioid sarcoma expresses cytokeratin consistently, CD34 in approximately half of the cases, and loses INI1 nuclear staining in all cases as a result of *SMARCB1* biallelic inactivation.[26] *SMARCB1* deficiency is mutually exclusive from inactivation of *SMARCA4*, which encodes for BRG1 (SMARCA4), another catalytic subunit of the SWI/SNF complex. SMARCA4-deficient malignant neoplasms, initially reported in the thoracic cavity,[27] have now been now recognized at many locations in the body,[28,29] and can also display rhabdoid features. The loss of BRG1 immunoreactivity represents a useful diagnostic marker. Another emerging class of malignant neoplasms that may be included in the differential diagnosis is the family of tumors with *NUTM1* gene rearrangements, formerly described mainly as *NUT*-midline carcinoma, but recently being found at various body sites including visceral organs and deep soft tissues and lacking convincing epithelial differentiation.[15,30,31] The latter cases of *NUTM1*-rearranged undifferentiated soft tissue and visceral tumors often display a round-epithelioid-rhabdoid phenotype arranged in solid sheets, nests and cords,[15] with strong and diffuse NUT nuclear immunopositivity, which is helpful in its diagnostic workup.[30] Additionally, the epithelioid-spindled morphology one of the cases (case 3), as well as its retroperitoneal location and loss of H3K27me3 immunostaining, raise the possibility of malignant peripheral nerve sheath tumor (MPNST).[32] However, MPNST has never been shown to harbor oncogenic fusions, and loss of H3K27me3, albeit a highly sensitive marker of MPNST, has been shown to lack specificity and could be seen in a wide range of mimics.[33]

Furthermore, a rare type of malignant epithelioid neoplasm characterized by the presence of *EWSR1/FUS::CREM* fusions was recently described having predilection for mesothelial-lined cavities, which can be an additional diagnostic consideration.[34] No specific immunoprofile is available to diagnose such tumors. Therefore, the use of molecular testing using a panel that covers common recurrent gene fusions may be useful for the workup of undifferentiated/poorly differentiated sarcomas. Finally, other poorly differentiated or dedifferentiated tumors should also be considered. Dedifferentiated liposarcoma is the top diagnostic consideration of any malignant mesenchymal tumors in the retroperitoneum but will show *MDM2/CDK4* amplification by genetic analysis.[35] Dedifferentiated melanoma—a melanoma that loses melanocytic markers expression including SOX10 and S100 and may resemble any other high-grade tumors—is a highly challenging diagnosis, and may require demonstration of an ultraviolet mutational signature or the presence of certain driver mutations, such as *BRAF* V600 and *NRAS* mutations in combination with a clinical history of melanoma to establish the diagnosis.[36–38]

In conclusion, we describe a series of *MAML2*-rearranged undifferentiated sarcomas with an epithelioid morphology and aggressive clinical behavior. Based on these findings, we recommend maintaining a high index of suspicion and suggest testing for potential oncogenic fusions when encountering an undifferentiated sarcoma with epithelioid morphology and monomorphic cytology, and inclusion of *MAML2* on targeted next-

generation fusion panels. Although a subset of our cases showed partial overlap with the recently described 'nodular necrotizing' variant of MIFS harboring *YAP1::MAML2* fusions, their pathogenetic relationship with the well-established family of MIFS remains unclear, given the low frequency of acral presentation and *VGLL3* upregulation/amplification, as well as the high rate of distant metastases. Further larger clinicopathologic studies with molecular correlates are needed to establish if *MAML2* gene rearrangements define a heterogeneous group of tumors or merely a wide morphologic spectrum of a single pathologic entity of soft tissue sarcomas with epithelioid phenotype.

Acknowledgement

We gratefully acknowledge the members of the Molecular Diagnostics Service in the Department of Pathology for their technical support.

Supported by:

P50 CA217694 (CRA), P30 CA008748 (CRA), Cycle for Survival (CRA), Kristin Ann Carr Foundation (CRA), Martin E Blackstein Research Fund (BCD), Panov 2 Research Program (BCD)

Funding Statement

This work was supported by P50 CA217694 (CRA), P30 CA008748 (CRA), Kristin Ann Carr Foundation (CRA). Martin E Blackstein Research Fund (BCD), Panov 2 Research Program (BCD). All other authors report no funding sources related to this study.

Data Availability Statement

Data sharing is not applicable to this article as no datasets were generated or analyzed during the current study.

References

1. Zema S, Pelullo M, Nardozza F, Felli MP, Screpanti I, Bellavia D. A dynamic role of mastermind-like 1: a journey through the main (path) ways between development and cancer. Front Cell Dev Biol 2020; 8: 613557. [PubMed: 33425921]
2. Wu L, Sun T, Kobayashi K, Gao P, Griffin JD. Identification of a family of mastermind-like transcriptional coactivators for mammalian notch receptors. Mol Cell Biol. 2002; 22(21): 7688–7700. [PubMed: 12370315]
3. Jin B, Shen H, Lin S, Li J, Chen Z, Griffin J, Wu L. The mastermind-like 1 (MAML1) coactivator regulates constitutive NF-kappaB signaling and cell survival. J Biol Chem. 2010; 285(19): 14356–14365. [PubMed: 20231278]
4. Alves-Guerra MC, Ronchini C, Capobianco AJ. Mastermind-like 1 is a specific coactivator of beta-catenin transcription activation and is essential for colon carcinoma cell survival. Cancer Res. 2007; 67(18): 8690–8698. [PubMed: 17875709]
5. Behboudi A, Enlund F, Winnes M, Andren Y, Nordkvist A, Leivo I, et al. Molecular classification of mucoepidermoid carcinomas-prognostic significance of the MECT1-MAML2 fusion oncogene. Genes Chromosomes Cancer. 2006; 45(5): 470–481. [PubMed: 16444749]
6. Sekine S, Kiyono T, Ryo E, Ogawa R, Wakai S, Ichikawa H, et al. Recurrent YAP1-MAML2 and YAP1-NUTM1 fusions in poroma and porocarcinoma. J Clin Invest. 2019; 129(9): 3827–3832. [PubMed: 31145701]
7. Vivero M, Davineni P, Nardi V, Chan JKC, Sholl LM. Metaplastic thymoma: a distinctive thymic neoplasm characterized by YAP1-MAML2 gene fusions. Mod Pathol. 2020; 33(4): 560–565. [PubMed: 31641231]

8. Perry KD, Al-Lbraheemi A, Rubin BP, Jen J, Ren H, Jang J, et al. Composite hemangioendothelioma with neuroendocrine marker expression: an aggressive variant. Mod Pathol. 2017; 30(11): 1589–1602. [PubMed: 28731049]
9. Antonescu CR, Dickson BC, Sung YS, Zhang L, Suurmeijer AJ, Stenzinger A, et al. Recurrent YAP1 and MAML2 rearrangements in retiform and composite hemangioendothelioma. Am J Surg Pathol. 2020; 44(12): 1677–1684. [PubMed: 32991341]
10. Dermawan JK, Westra WH, Antonescu CR. Recurrent PTBP1::MAML2 fusions in composite hemangioendothelioma with neuroendocrine differentiation: a report of two cases involving neck lymph nodes. Genes Chromosomes Cancer. 2022; 61(4): 187–193. [PubMed: 34862698]
11. Perret R, Tallegas M, Velasco V, Soubeyran I, Coindre JM, Azmani R, Baud J, Bacle G, De Pinieux G, Le Loarer F. Recurrent YAP1::MAML2 fusions in “nodular necrotizing” variants of myxoinflammatory fibroblastic sarcoma: a comprehensive study of 7 cases. Mod Pathol 2022; 35(10): 1398–1404.arbaji [PubMed: 35546636]
12. Cheng DT, Mitchell TN, Zehir A, Shah RH, Benayed R, Syed A, et al. Memorial Sloan Kettering-Integrated Mutation Profiling of Actionable Cancer Targets (MSK-IMPACT): A Hybridization Capture-Based Next-Generation Sequencing Clinical Assay for Solid Tumor Molecular Oncology. J Mol Diagn 2015; 17(3), 251–264. [PubMed: 25801821]
13. Zheng Z, Liebers M, Zhelyazkova B, Cao Y, Panditi D, Lynch KD, et al. Anchored multiplex PCR for targeted next-generation sequencing. Nat Med 2014; 20(12): 1479–1484. [PubMed: 25384085]
14. Benayed R, Offin M, Mullaney K, Sukhadia P, Rios K, Desmeules P, et al. High yield of RNA sequencing for targetable kinase fusions in lung adenocarcinomas with no mitogenic driver alteration detected by DNA sequencing and low tumor mutation burden. Clin Cancer Res 2019; 25(15): 4712–4722. [PubMed: 31028088]
15. Dickson BC, Sung YS, Rosenblum MK, Reuter VE, Harb M, Wunder JS, Swanson D, Antonescu CR. NUTM1 Gene Fusions Characterize a Subset of Undifferentiated Soft Tissue and Visceral Tumors. Am J Surg Pathol 2018; 42(5): 636–645. [PubMed: 29356724]
16. Dickson BC, Swanson D. Targeted RNA sequencing: a routine ancillary technique in the diagnosis of bone and soft tissue neoplasms. Genes Chromosomes Cancer 2019; 58(2): 75–87. [PubMed: 30350361]
17. Kim J, Kwon H, Shin YK, Song G, Lee T, Kim Y, et al. MAML1/2 promote YAP/TAZ nuclear localization and tumorigenesis. Proc Natl Acad Sci U S A 2020; 117(24): 13529–13540. [PubMed: 32482852]
18. Anderson WJ, Fletcher CDM, Hornick JL. Loss of expression of YAP1 C-terminus as an ancillary marker for epithelioid hemangioendothelioma variant with YAP1-TFE3 fusion and other YAP1-related vascular neoplasms. Mod Pathol 2021; 34(11): 2036–2042. [PubMed: 34148063]
19. Antonescu CR, Zhang L, Nielsen GP, Rosenberg AE, Dal Cin P, Fletcher CDM. Consistent t(1;10) with rearrangements of TGFBR3 and MGEA5 in both myxoinflammatory fibroblastic sarcoma and hemosiderotic fibrolipomatous tumor. Genes Chromosomes Cancer 2011; 50(10): 757–764. [PubMed: 21717526]
20. Hallor KH, Sciot R, Staaf J, Heidenblad M, Rydholm A, Bauer HC, et al. Two genetic pathways, t(1;10) and amplification of 3p11–12 in myxoinflammatory fibroblastic sarcoma, hemosiderotic fibrolipomatous tumors, and morphologically similar lesions. J Pathol. 2009; 217(5): 716–727. [PubMed: 19199331]
21. Arbajian E, Hofvander J, Magnusson L, Mertens F. Deep sequencing of myxoinflammatory fibroblastic sarcoma. Genes Chromosomes Cancer 2020; 59(5): 309–317. [PubMed: 31898851]
22. Suster D, Michal M, Huang H, Ronen S, Springborn S, Debiec-Rychter M, et al. Myxoinflammatory fibroblastic sarcoma: an immunohistochemical and molecular genetic study of 73 cases. Mod Pathol. 2020; 33(12): 2520–2533. [PubMed: 32514165]
23. Kao YC, Ranucci V, Zhang L, Sung YS, Athanasian EA, Swanson D, et al. Recurrent BRAF gene rearrangements in myxoinflammatory fibroblastic sarcomas, but not hemosiderotic fibrolipomatous tumors. Am J Surg Pathol. 2017; 41(11), 1456–1465. [PubMed: 28692601]
24. Hélias-Rodzewicz Z, Pérot G, Chibon F, Ferreira C, Lagarde P, et al. YAP1 and VGLL3, encoding two cofactors of TEAD transcription factors, are amplified and overexpressed in a subset of soft tissue sarcomas. Genes Chromosomes Cancer 2010; 49(12): 1161–1171. [PubMed: 20842732]

25. Cancer Genome Atlas Research Network. Comprehensive and Integrated Genomic Characterization of Adult Soft Tissue Sarcomas. Cell 2017; 171(4): 950–965.e28. [PubMed: 29100075]
26. Le Loarer F, Zhang L, Fletcher CD, Riberiro A, Singer S, Italiano A, et al. Consistent SMARCB1 homozygous deletions in epithelioid sarcoma and in a subset of myoepithelial carcinomas can be reliably detected by FISH in archival material. Genes Chromosomes Cancer 2014; 53(6): 475–486. [PubMed: 24585572]
27. Sauter JL, Graham RP, Larsen BT, Jenkins SM, Roden AJ, Bolan JM. SMARCA4-deficient thoracic sarcoma: a distinctive clinicopathologic entity with undifferentiated rhabdoid morphology and aggressive behavior. Mod Pathol. 2017; 30: 1422–1432. [PubMed: 28643792]
28. Agaimy A, Jain D, Uddin N, Rooper LM, Bishop JA. SMARCA4-deficient Sinonasal Carcinoma: A Series of 10 Cases Expanding the Genetic Spectrum of SWI/SNF-driven Sinonasal Malignancies. Am J Surg Pathol. 2020; 44(5): 703–710. [PubMed: 31934917]
29. Horton RK, Ahadi M, Gill AJ, Said S, Chen ZE, Bakhshwin A, et al. SMARCA4/SMARCA2-deficient Carcinoma of the Esophagus and Gastroesophageal Junction. Am J Surg Pathol. 2021; 45(3): 414–420. [PubMed: 33027072]
30. Stevens TM, Morlote D, Xiu J, Swensen J, Brandwin-Weber M, Miettinen M, et al. NUTM1-rearranged neoplasia: a multi-institution experience yields novel fusion partners and expands the histologic spectrum. Mod Pathol. 2019; 32(6): 764–773. [PubMed: 30723300]
31. Van Treeck BJ, Thangaiah JJ, Torres-Mora J, Stevens TM, Rothermundt C, Fassan M, et al. NUTM1-rearranged colorectal sarcoma: a clinicopathologically and genetically distinctive malignant neoplasm with a poor prognosis. Mod Pathol. 2021; 34(8): 1547–1557. [PubMed: 33714983]
32. Prieto-Granada CN, Wiesner T, Messina JL, Jungbluth AA, Chi P, Antonescu CR. Loss of H3K27me3 Expression Is a Highly Sensitive Marker for Sporadic and Radiation-induced MPNST. Am J Surg Pathol. 2016; 40(4): 479–489. [PubMed: 26645727]
33. Le Guellec S, Macagno N, Velasco V, Lamant L, Lae M, Filleron T, et al. Loss of H3K27 trimethylation is not suitable for distinguishing malignant peripheral nerve sheath tumor from melanoma: a study of 387 cases including mimicking lesions. Mod Pathol. 2017; 30(12): 1677–1687. [PubMed: 28752843]
34. Argani P, Harvey I, Nielsen GP, Takano A, Suurmeijer AJH, Voltaggio L, et al. EWSR1/FUS-CREB fusions define a distinctive malignant epithelioid neoplasm with predilection for mesothelial-lined cavities. Mod Pathol. 2020; 33(11): 2233–2243. [PubMed: 32770123]
35. Dal Cin P, Kools P, Sciot R, WEver ID, Van Damme B, Van de Ven W, Van den Berghe H. Cytogenetic and fluorescence in situ hybridization investigation of ring chromosomes characterizing a specific pathologic subgroup of adipose tissue tumors. Cancer Genetics Cytogenet. 1993; 68(2): 85–90.
36. Alrabadi N, Gibson N, Curless K, Cheng L, Kuhar M, Chen S, et al. Detection of driver mutations in *BRAF* can aid in diagnosis and early treatment of dedifferentiated metastatic melanoma. Mod Pathol. 2019; 32(3): 330–337. [PubMed: 30315274]
37. Yang C, Sanchez-Vega F, Chang JC, Chatila WK, Shoushtari AN, Ladanyi M, et al. Lung-only melanoma: UV mutational signature supports origin from occult cutaneous primariers and argues against the concept of primary pulmonary melanoma. Mod Pathol. 2020; 33(11): 2244–2255. [PubMed: 32581366]
38. Agaimy A, Stoehr R, Hornung A, Popp J, Erdmann M, Heinzerling L, Hartmann A. Dedifferentiated and Undifferentiated Melanomas: Report of 35 New Cases with Literature Review and Proposal of Diagnostic Criteria. Am J Surg Pathol. 2021; 45(2): 240–254. [PubMed: 33428337]
39. Gu Z, Gu L, Eils R, Schlesner M, Brors B. circlize Implements and enhances circular visualization in R. Bioinformatics 2014; 30(19): 2811–2812. [PubMed: 24930139]

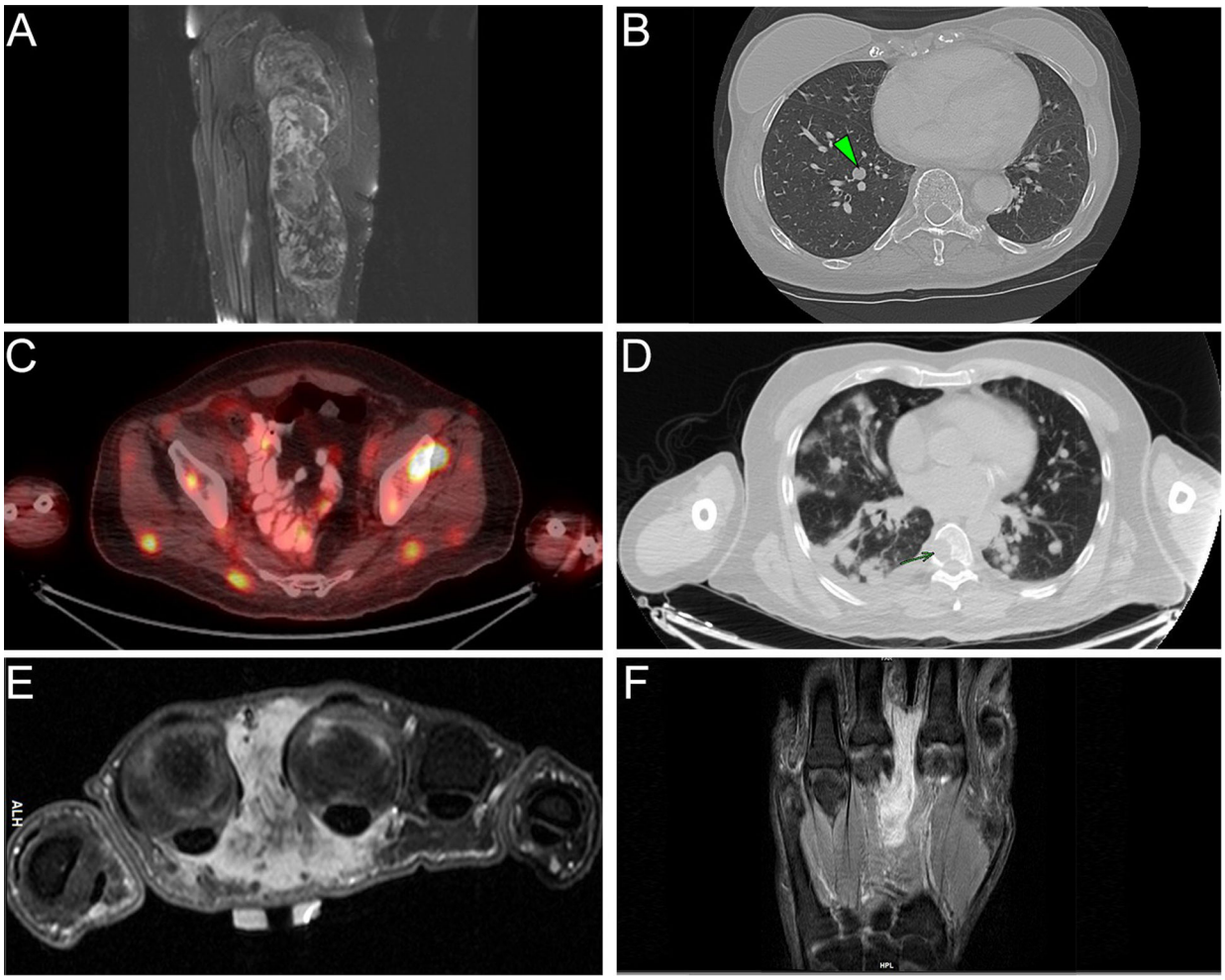

Figure 1. Radiologic presentation.

A, Magnetic resonance imaging (MRI) showing a sagittal view of a large thigh mass involving the left hip and abductor musculature (T2-weighted sequence with fat suppression) (case 1). **B**, Computed tomography (CT) imaging showing a transverse view of right lower lobe metastases (green arrowhead) from the thigh mass (case 1). **C**, Positron emission tomography (PET) imaging showing multifocal FDG-avid tumors involving the abdominal wall skeletal muscles and adipose tissue (case 2). **D**, CT imaging showing extensive bilateral lung metastases (case 2). **E-F**, MRI showing the axial (T1-weighted, fat suppressed) and coronal (T2-weighted) views of an infiltrative tumor involving subcutaneous tissue and skeletal muscle between the 2nd and 3rd digits of the left hand (case 4).

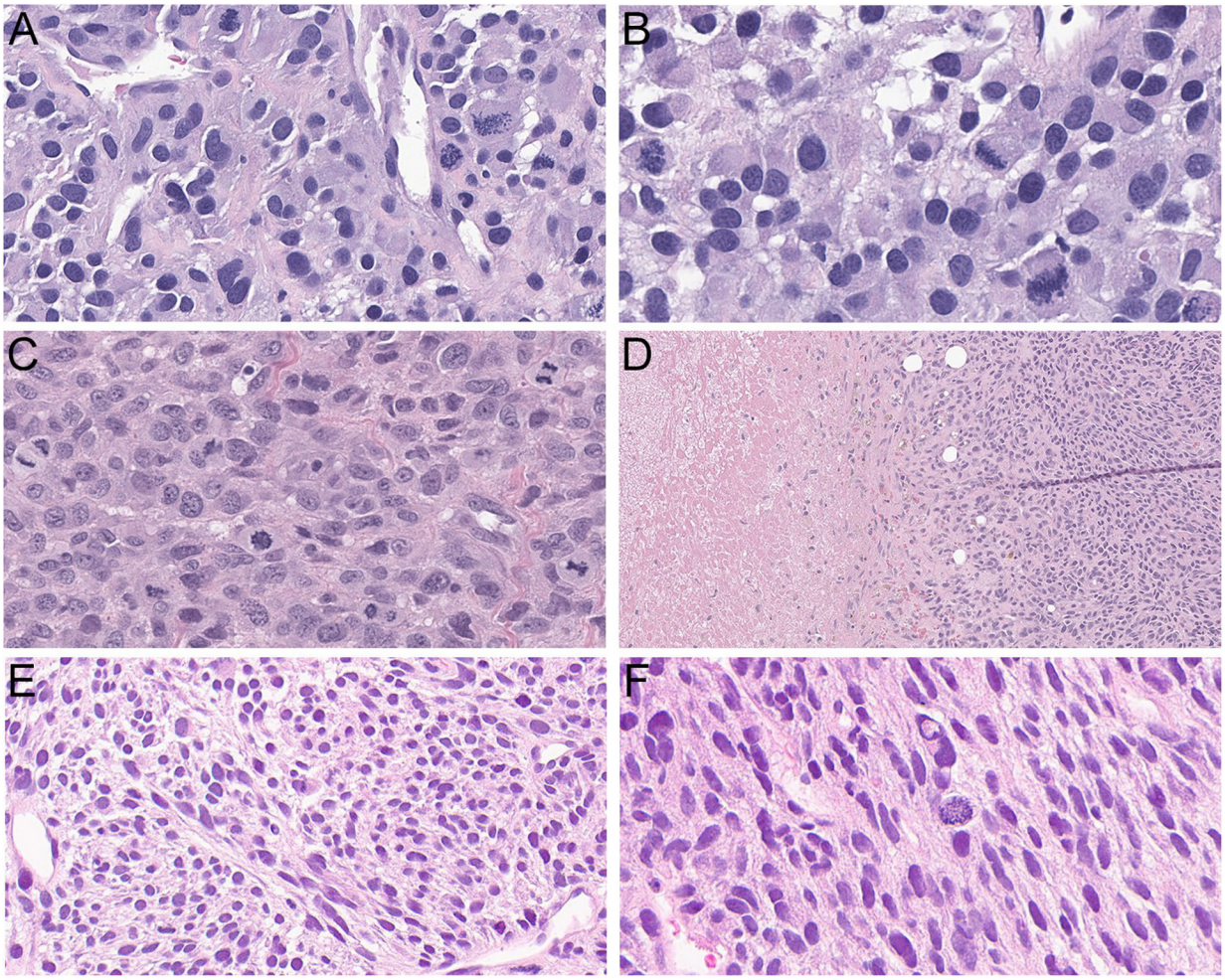

Figure 2. Histologic features (cases 1–3).

A,B, Cellular epithelioid neoplasm showing tumor cells arranged in solid sheets and nests and displaying round to ovoid nuclei, even chromatin, abundant amphophilic cytoplasm and brisk mitotic activity (case 1; A, B: 400X). **C,D**, Malignant epithelioid neoplasm showing tumor cells arranged in solid sheets with mild to moderate nuclear pleomorphism, prominent nucleoli, frequent mitotic figures, and extensive tumor necrosis (case 2; C: 400X, D: 100X). **E,F**, Cellular epithelioid and spindled neoplasm showing tumor cells arranged in nests and solid sheets and with ovoid, tapering nuclei, pale eosinophilic cytoplasm, and readily identifiable mitotic figure (case 3; E: 200X, F: 400X). A-F: hematoxylin & eosin.

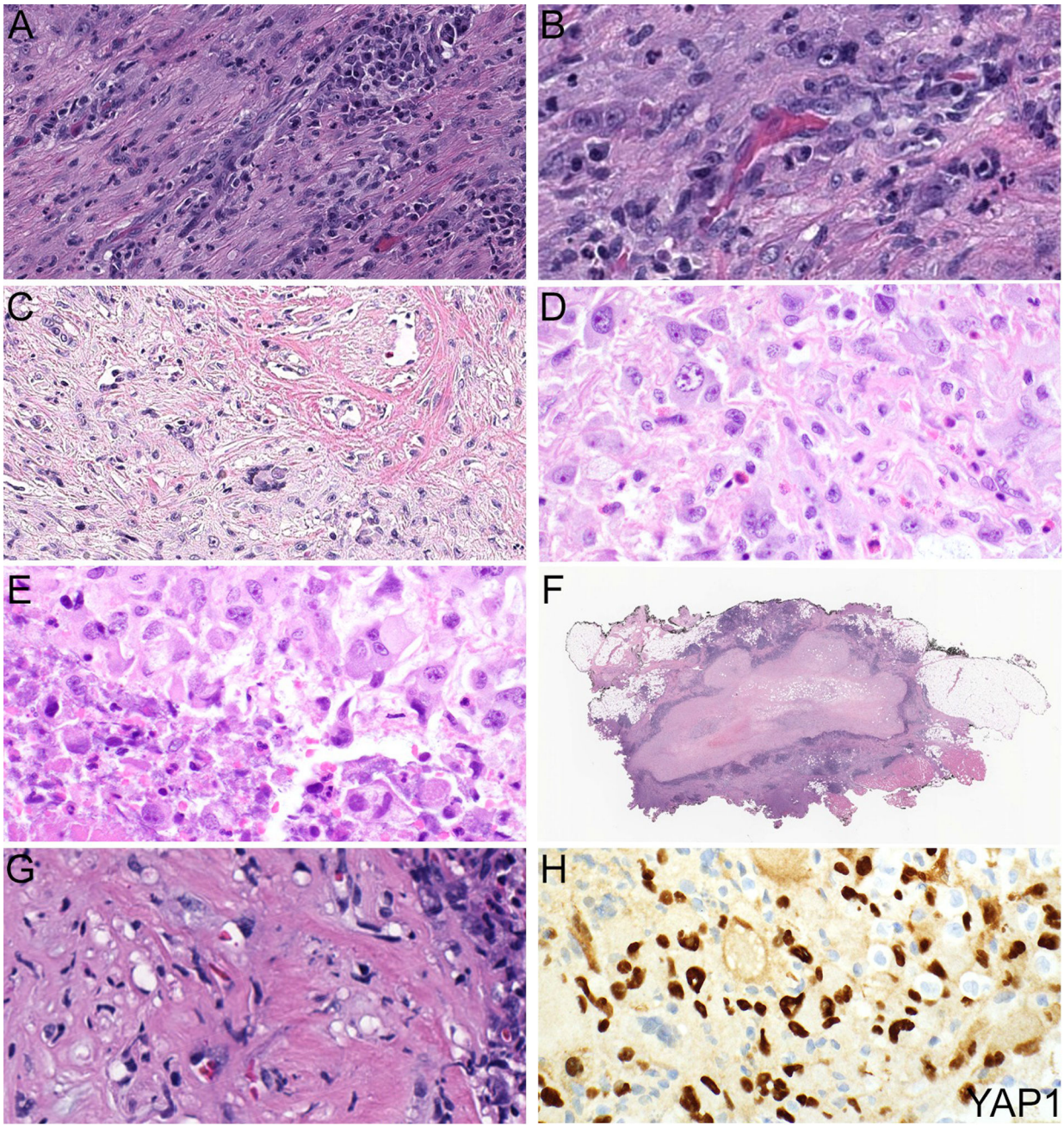

Figure 3. Histologic features (cases 4–6).

A, B, Pleomorphic epithelioid neoplasm showing tumor cells with prominent macronucleoli and admixed with a neutrophilic and lymphoplasmacytic infiltrate (case 4; A: 200X, B: 400X). **C**, Scattered punctate necrosis and touton-like giant cells are present (case 4, 200X). **D**, Epithelioid neoplasm showing tumor cells with prominent macronucleoli and abundant eosinophilic cytoplasm, admixed with eosinophils (case 5, 400X). **E**, Extensive tumor necrosis is present (case 5, 400X). **F, G**, Epithelioid/histiocytoid cells set in extensively hyalinized/necrotic tissue rimmed by lymphoid tissue (case 6: **F**, whole slide image;

G, 400X). **H**, YAP1 immunohistochemistry showing overexpression of YAP1 nuclear immunostaining (case 5, 400X) A-G: hematoxylin & eosin.

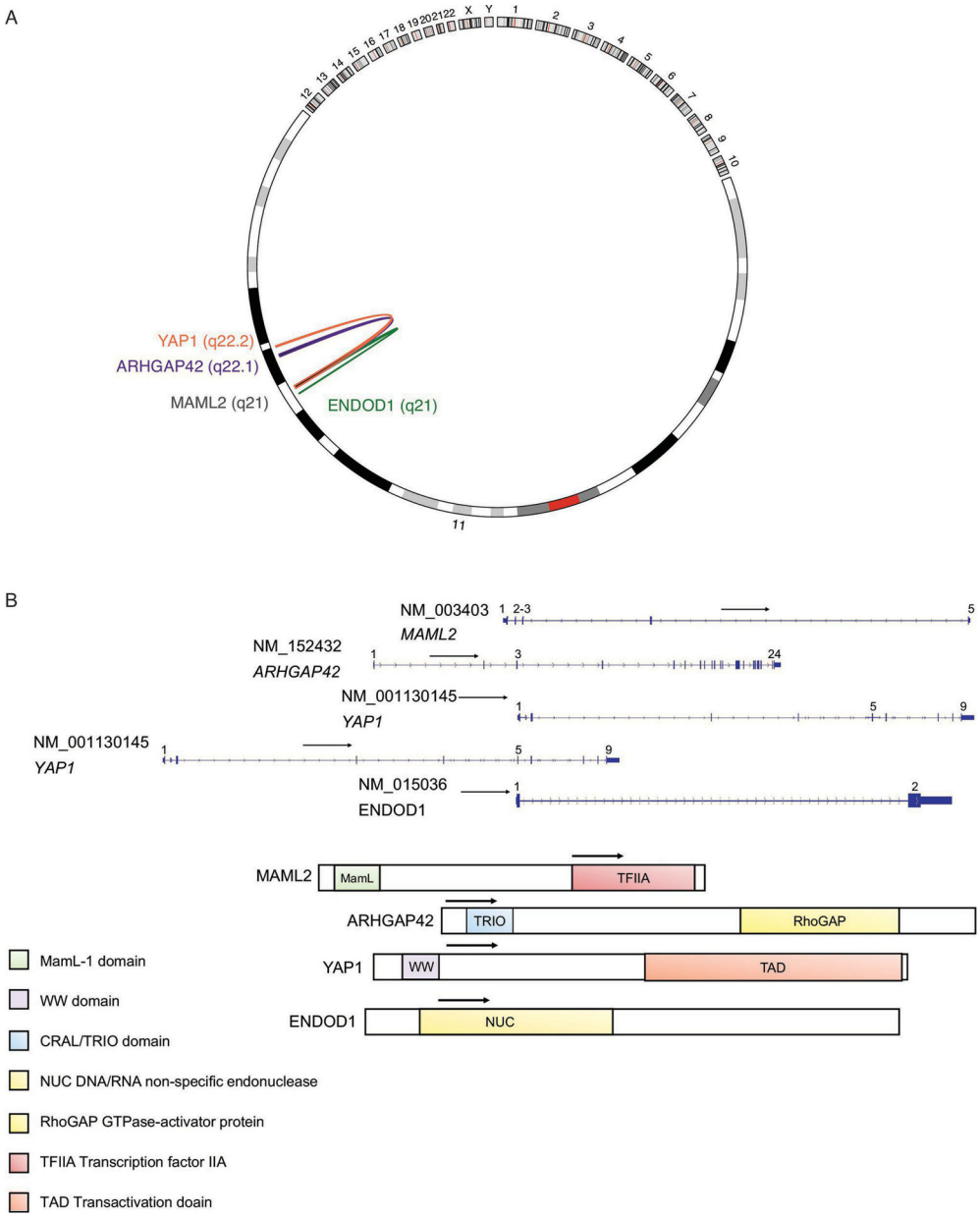

Figure 4. *MAML2* fusions schematic diagrams.

A: Circos plot depicting *MAML2* fusions represented by links between cytobands (hg19 genome). Plot generated using R package "circlicize" version 0.4.13.[39] **B**: Schematic of *MAML2* fusion transcripts annotated by NCBI RefSeq accession numbers. Numbers and black arrows represent exons and directions of transcript, respectively. Predicted chimeric proteins with protein domains are depicted below the transcripts. Horizontal black arrows designate portions of the protein domains that are present in the chimeric protein. Vertical dotted red line represents fusion breakpoint.

Table 1.

Clinical Summary

Case	Age (years)	Sex	Site	Greatest dimension (cm)	Presentation	Treatment	Status at last follow-up	Follow-up period (months)
1	70	Female	Left hip involving abductor musculature.	11.5	Large thigh mass for 1 year	Wide resection followed by adjuvant chemotherapy for metastatic disease	AWD (metastases to lung)	8
2	71	Male	Multifocal abdominal wall tumors involving skeletal muscles and adipose tissue	Multiple, 2.0 cm in greatest dimension	Multifocal subcutaneous abdominal nodules multiplied and spread to back. Progressive dyspnea	Chemotherapy (decitabine, docetaxel)	DOD (metastases to lung, soft tissue, bone)	2
3	65	Male	Retroperitoneum	14.8	Large retroperitoneal mass on imaging	Neoadjuvant radiation therapy, surgical resection		
4	56	Male	Left hand subcutaneous tissue and skeletal muscle	4.5	Pain and mass in left hand for 1 year	2-ray amputation	ANED	36
5	48	Male	Left knee	5.0	Large left knee soft tissue mass	Local radiotherapy and systemic chemotherapy	AWD (metastases to lung)	5
6	41	Male	Left arm	1.3	Painful, enlarging lump for 3–4 months	Biopsy followed by excision	ANED	2

ANED: alive with no evidence of disease; AWD: alive with disease; DOD: dead of disease.

Table 2.

Histopathologic Findings

Case	Histology	Cytomorphology	Mitoses (per 10 HPF)	Necrosis
1	Solid sheets; UPS-like	High grade, pleomorphic spindled and epithelioid cells with hyperchromatic chromatin and abundant amphophilic cytoplasm	17	Focal
2	Solid sheets; malignant epithelioid neoplasm	High grade epithelioid cells with abundant amphophilic cytoplasm and prominent nucleoli	> 20	Extensive
3	Malignant epithelioid to spindle cell neoplasm in a fascicular-herringbone pattern; occasional ectatic and branching thin-walled vessels	Ovoid to epithelioid cells with mild pleomorphism, pale and eosinophilic cytoplasm	> 20	Focal
4	MIFS-like: Sheets of plump histiocytoid cells and rare virocyte-like large cells admixed with an eosinophilic and lymphoplasmacytic infiltrate; myxoid to collagenous stroma; diffusely infiltrative growth; occasional touton like giant cells	Plump histiocytoid cells with pale eosinophilic to foamy cytoplasm and round nuclei; occasional large cells with vesicular chromatin and enlarged virocyte-like nucleoli	3	Focal
5	MIFS-like: Sheets of plump histiocytoid cells and rare virocyte-like large cells admixed with a lymphoplasmacytic infiltrate	Predominantly composed of histiocytes and lymphoplasmacytic infiltrate. Admixed rare large cells with prominent nucleoli	> 20	Extensive
6	Malignant neoplasm composed of sheets and clusters of atypical epithelioid/histiocytoid cells against extensively hyalinized/necrotic tissue rimmed by lymphoid tissue	Spindled to epithelioid/histiocytoid cells with atypical, hyperchromatic, irregular nuclei with pink, vacuolated cytoplasm	< 1	Extensive (necrosis/ hyalinization)

HPF: high power fields; MIFS: myxoinflammatory fibroblastic sarcoma; UPS: undifferentiated pleomorphic sarcoma.

Table 3.

Immunohistochemical (IHC) and Molecular Findings

Case	IHC (+)	IHC (−)	5' Gene	3' Gene	Additional Molecular Findings
1	SMA, caldesmon, CK OSCAR (rare)	pan-CK, EMA, CK7, S100, SOX10, HMB45, MDM2, CDK4, Desmin, CD163, CD31, ERG, CD3, CD20, CD45, CD117, DOG1, pan-NTRK, MUC4, ALK, Mel-A, TFE3. INI1, BRG1 and BRM retained.	*ARHGAP42* (NM_152432) exon 3	*MAML2* (NM_003403.4) exon 3	*TP53* p.Y234C, *PTEN* intragenic deletion, *RB1* p.A538Qfs*5, *BRCA2* p.A2351P, *HNF1A* p.A534T, *PREX2* p.N64T. TMB 4.1 mt/Mb. mRNA expression: *MAML2* and *VGLL3* expression levels not upregulated.
2	PDGFRB 4+, vimentin	AE1/AE3, CAM5.2, CK5/6, CK7, CK20, EMA, PSA, Mart-1, S-100, p63, TTF-1, SMA, desmin, myogenin, WT1, MUM1, CD34, ALK (D5F3), NUT, and pan-NTRK. CD45, CD56, CD34, CD20, ERG, CD117, CD21, SF-1, SOX10 and BRAF VE1. INI1, BRG1 and H3K27me3 (retained)	*ENDOD1* (NM_015036) exon 1	*MAML2* (NM_003403.4) exon 3	19p13.2 amplification (*CCNE1*, *BRD4*, *NOTCH3*), 9p21.3 deletion (*CDKN2A*/*CDKN2B*), point mutations including *PDGFRB* hotspot exon 11 p.1547_1553dup and exon 18 p.R853P. TMB 6.6 mt/Mb. mRNA expression: *MAML2* and *VGLL3* expression levels not upregulated.
3	Desmin (focal), DOG1 (patchy weak), loss of H3K27me3	AE1/AE3, SMA, myogenin, S100, SOX10, HMB45, CD34 MDM2	*ARHGAP42* (NM_152432) exon 2	*MAML2* (NM_003403.4) exon 2	
4	CD68 (KP1 and PGM1) and CD163 in histiocytes, pan-cytokeratin (rare cells), TFE3	EMA, 34BE12, HMB45, CD15, CD30, cathepsin-K, ALK-D5F3, S100, CD1a, langerin, CD31, CD34, ERG, EMA, desmin BRAF VE1. INI-1 (retained)	*YAP1* (NM_001130145) exon 5	*MAML2* (NM_003403.4) exon 2	mRNA expression: *MAML2* not upregulated.
5	YAP1, AE1/AE3, D2–40, SMA (focal), EMA (focal)	ERG, CD34, desmin, S100, HMB-45, Melan-A, MITF, SOX10, MyoD1. INI-1 (retained)	*YAP1* (NM_001130145) exon 1	*MAML2* (NM_003403.4) exon 2	*RBMS3* (NM_014483.3) exon 11::*RAF1* (NM_002880.3) exon 8. mRNA expression: *VGLL3* upregulated; *MAML2* not upregulated.
6	AE1/AE3, S100	EMA, p63, ERG, SOX10, INI1 (retained)	*YAP1* (NM_001130145) exon 5	*MAML2* (NM_003403.4) exon 2	mRNA expression: *MAML2, VGLL3* and *YAP1* not upregulated.